

## SYNTHESIS OF RESULTS FOR THE TEE-JUNCTION BENCHMARK

John Mahaffy  
WheelSmith Farm, USA

### ***Introduction***

Because of the relatively large number of benchmark submissions, an extremely large number of possible comparisons with data and between submissions are possible. As a result data reduction and plotting were all accomplished with a Python script to control the total level of effort. In the end most of the man-hours expended in this synthesis dealt with initial problems in the submissions and trying to make sense of the plots produced by the script.

The range of observations made during the synthesis was restricted by two factors. The work was a part-time, unpaid effort by a single individual, and within the context of CFD the amount of information available for analysis was relatively small. Anyone wanting a more detailed picture of the benchmark than presented here should also read the detailed description of experimental results and papers produced by benchmark participants.

### ***Available Data***

All data presented in this paper is property of Vattenfall Research and Development AB and has been used with their permission.

Vattenfall provided time averaged temperature and temperature fluctuations for all thermocouples. They are located at 0°, 90°, 180°, and 270°, two, four, six, eight, and ten hydraulic diameters downstream of the tee junction, and at 0° and 180°, fifteen and twenty hydraulic diameters downstream of the tee junction. In addition time dependent temperature readings were provided two and four hydraulic diameters downstream of the tee junction at the four angular locations, at 0°, 180°, and 270° six diameters downstream, and at 0°, 90°, and 180° eight diameters downstream. This data was collected every five milliseconds for three hundred seconds.

Vattenfall provided PIV data at 1.6, 2.6, 3.6, and 4.6 hydraulic diameters downstream of the tee junction. Time averaged and RMS fluctuations were provided for the x and z velocity components (U and W) along a vertical line through the center of the pipe at the four x locations. Time averaged and RMS fluctuations were provided for the x and y velocity components (U and V) along a horizontal line through the center of the pipe at the same four x locations. Reynolds stresses were also provided along these lines. The number of values provided for each velocity component on each line varied a bit, but was roughly 35.

Time dependent PIV information was provided at the same four downstream locations, but only for a restricted number of points. All three velocity components were provided on the pipe centerline. The x and z components (U and W) were provided at  $y=0$  and  $z = \pm 35\text{mm}$ , and the x and y components provided at  $z=0$  and  $y = \pm 35\text{mm}$ . PIV data was sampled 60 times

per second for 12 seconds, and two independent 12 second samples were provided for each velocity component at each location. Time duration was limited by storage capacity for the digital images.

Because of the PIV data's sparsity, standard visualization techniques cannot be applied to characterize flow oscillations resulting from the side leg injection. However, Fourier analysis of the transient thermocouple and PIV data provides useful information for comparison with transient CFD results. Fourier spectra from both data and CFD tend to be noisy, so all results presented in this paper have been smoothed with a running average from five results before to five results after the actual result at a given time.

For experiments in the same facility with flow ratios (cold inlet volumetric flow divided by hot inlet volumetric flow) of 1 and 2, Odemark et. al report peaks in the temperature transforms at 3 Hz and 4 Hz respectively. The flow ratio for this benchmark is 1.5 and discrete Fourier transforms of thermocouple data at  $x=2D$ ,  $270^\circ$ ,  $x=4D$ ,  $90^\circ$  and  $270^\circ$  show a distinct peak at approximately 3.5 Hz (e.g. Figure 1). Weaker peaks are visible in transforms of transient data from thermocouples at  $x=2D$ ,  $90^\circ$ , and  $x=6D$ ,  $270^\circ$ . No other thermocouple data showed this peak.

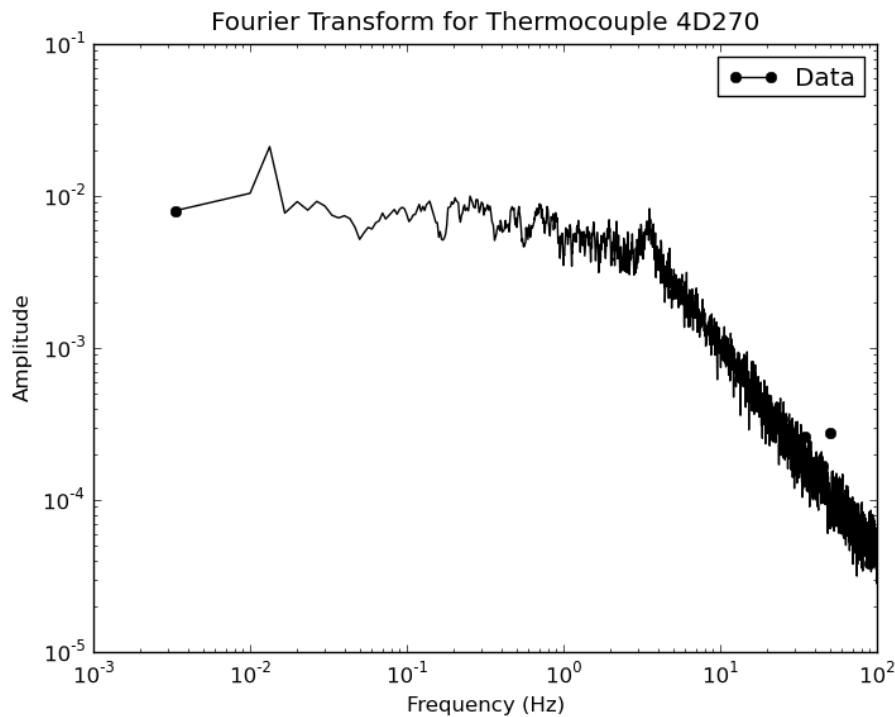


**Figure 1 Thermocouple Spectrum at  $x=4D$ ,  $270^\circ$**

Since the velocity field drives the temperature distribution, peaks are expected, and found, in transforms of some of the PIV data. Strong peaks are seen around 3.5 Hz at all four downstream locations for U (x component) at  $z=0$  and  $y = \pm 35\text{mm}$  and for V (y component) on the centerline (see Figure 2 and Figure 3). Strong peaks are also seen for V 3.6 and 4.6 hydraulic diameters downstream of the junction at  $z=0$  and  $y = \pm 35\text{mm}$ . Weak peaks appear

to be present for U on the centerline at all four x locations and at  $y=0$ ,  $z = \pm 35\text{mm}$  for  $x = 3.6D$  and  $4.6D$ .

There is some indication of organized oscillations in the range of 4-6 Hz, and below 1 Hz. However, short duration of the PIV samples and the weak and infrequent occurrence of peaks above 4 Hz do not justify any conclusions at this time.

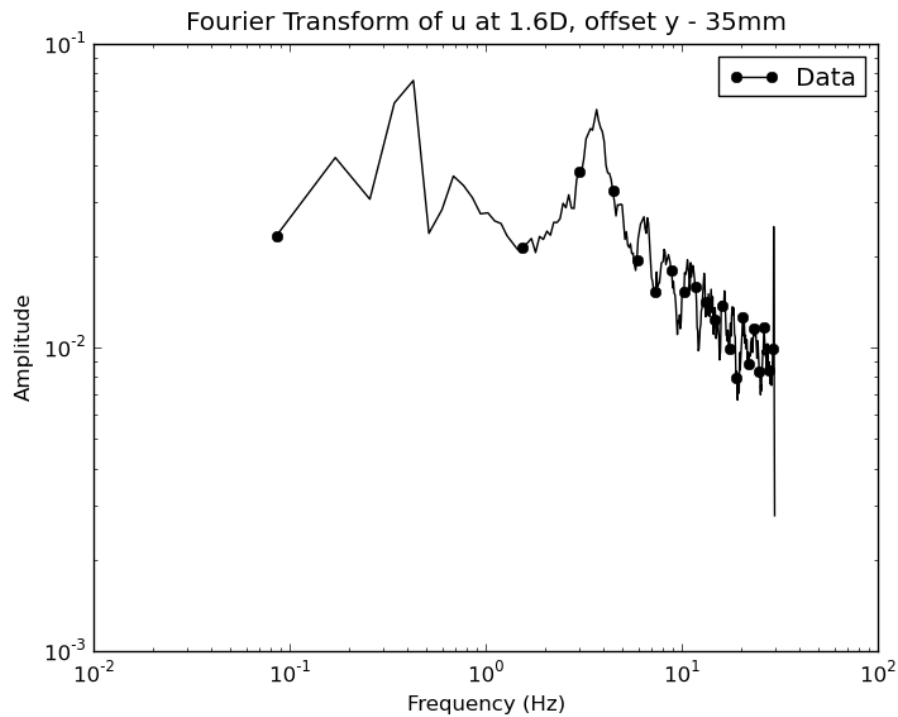


**Figure 2 Velocity x-component Spectrum at  $x=1.6D$ ,  $y=-35\text{mm}$ ,  $z=0$**

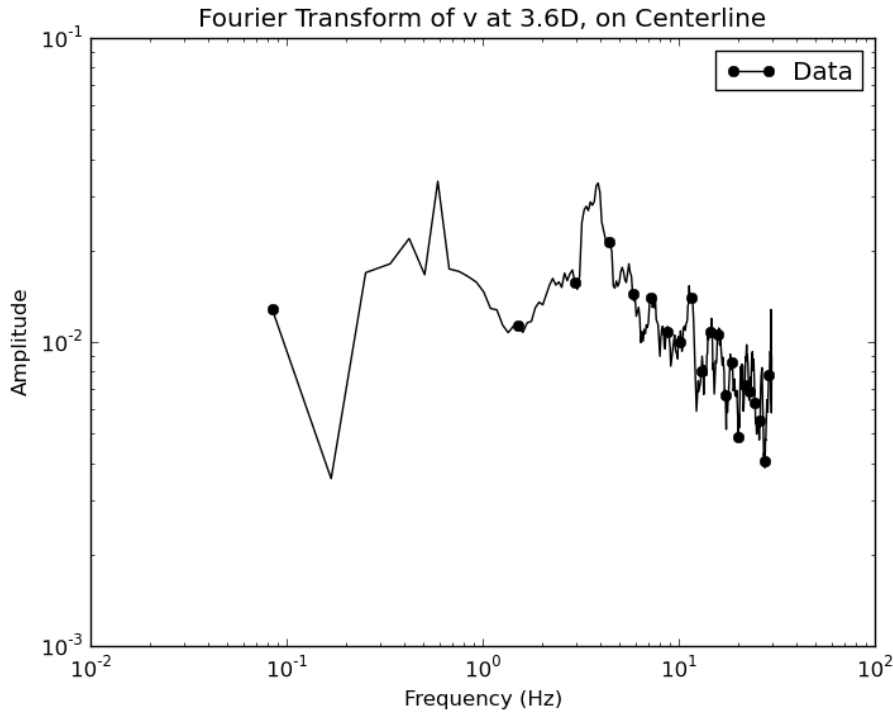


**Figure 3 Velocity y-component Spectrum at  $x=3.6D$ ,  $y=0$ ,  $z=0$**

### ***Simple Metric for Comparison***

Given the relatively large number of submissions and even larger number of possible comparisons between experiment and calculation, a good starting point was needed for the synthesis of results. A very simple metric was chosen to quickly compare the relative quality of the CFD calculations. For any given curve (e.g. x component of velocity along a vertical line through the pipe center) the metric is defined as:

$$M = \frac{1}{N} \sum_{i=1, N} |C_i - D_i| ,$$

where N is the total number of CFD results in the curve,  $C_i$  is the  $i^{\text{th}}$  result from the CFD calculation and  $D_i$  is the experimental data at the same location. In cases where reported CFD and experimental results are not co-located, a simple linear interpolation is applied to the experimental data to get an estimated value at the location of the specific CFD result.

These metrics were generated for all benchmark submissions using all comparisons of time averaged velocity components, RMS velocity fluctuations, time averaged temperatures, and RMS temperature fluctuations. No attempt was made to compare time dependent results in this way.

Ranking of submissions was done separately for comparisons related to velocities and for those related to temperatures. For each application of the metric the 29 submissions were assigned a rank from 1 (lowest metric value) to 29 (highest metric value). After all comparisons were completed, those associated with velocities were summed to provide one summary score and those associated with temperature were summed for a second summary score. The ranking of time averaged y-component of velocity was not included in the final score. Because of the symmetry plane in the experiment, this time average should in theory be zero. However, in practice, small non-zero values should be expected, and Figure 4 suggests that small unreported asymmetries in the experiment result in non-zero values.

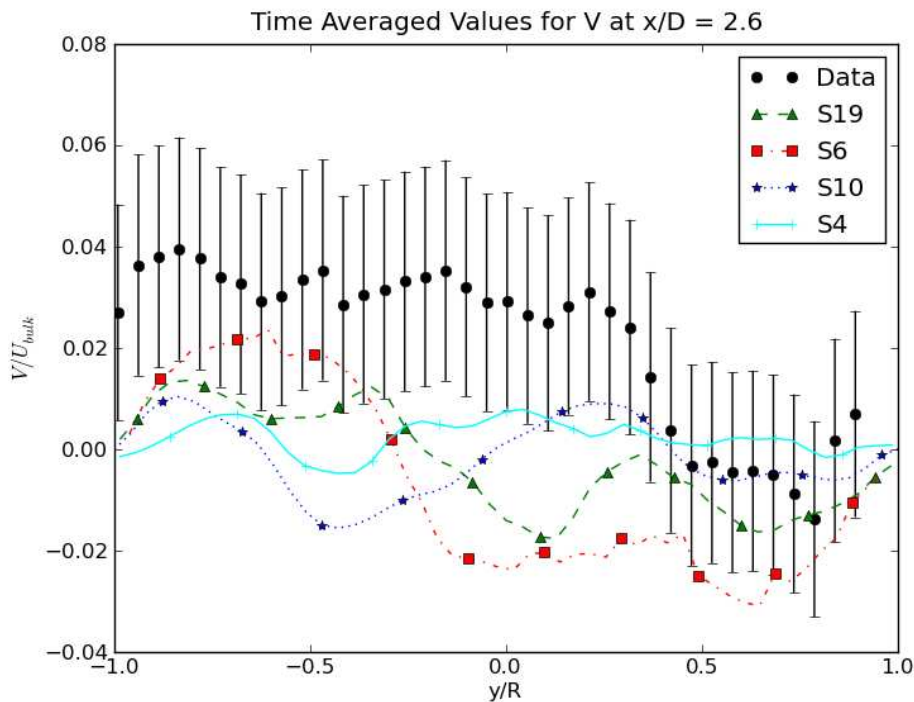


**Figure 4: Time Averaged y-component of Velocity at  $x = 2.6D$**

The final ranking for velocity based comparisons is shown in Table 1 and ranking based upon temperature comparisons is shown in Table 2. A lower score is a better result, but remember that the ranking method was just intended as a rough way to extract useful information from the results. Better metrics are available, and with some study, better ways of weighting the metrics between data sets could be constructed.

Detailed conclusions are not possible without a detailed review of nodalizations. However, at least two features stand out immediately for the velocity based comparisons. For the same selection of turbulence model, total number of discrete volumes is generally a good indicator of quality. This suggests that most participants were reasonably careful in their selection of mesh within the constraints of available computer resources. Also, for roughly the same number of volumes, the SAS-SST appears to be significantly under-performing LES with Dynamic Smagorinsky or WALE. Other results show that SST is performing well, so

problems with quality of results are probably due to SAS. This is explored in more detail below.

**Table 1 Submissions Ranked by Comparison to PIV Data**

<b>Submission</b>	<b>Velocity Score</b>	<b>Code</b>	<b>Turbulence</b>	<b>Volumes</b>
S20	75	FLUENT	LES, Dyn. Smagorinsky	70.5M
S2	166	Fluent 12	LES, Dyn. Smagorinsky	34M
S8	178	STAR-CCM+/3.06.006	LES-Wale SGS	13.2 M
S4	184	Fluent 6.3.26	LES, Dyn. Smagorinsky	5.8M
S24	212	OpenFOAM 1.6	LES, Dyn. Smagorinsky	8 M
S21	247	Nek5000	LES, spectral damping	21M
S16	270	Fluent 12	LES-WALE	7.7M
S3	311	CFX5 v12	LES, WALE	0.97M
S11	312	CFX	LES-Wale	3.4M
S19	322	FLUENT 12.1	SST-kw	11M
S18	349	CFX	DES-SST	2.4M
S14	358	CABARET	ILES	1.8M
S17	374	OpenFOAM 1.6	LES, 1eqn. Dyn. eddy	0.28M
S9	375	Advance/FrontFlow/red v4	LES-Smagorinsky	4.1 M
S22	404	Star-CCM+	LES	4.4 M
S6	408	STAR-CCM+/3.06.006	LES-Wale	9.3 M
S26	432	FLUENT v12.1	LES - Dynamic KE SGS	7.2 M
S27	446	STAR-CCM+	V <sup>2</sup> F	0.62 M
S23	458	CFX	LES-WALE	1.9 M
S10	477	Fluent 12	LES-Smagorinsky-Lilly	0.92M
S5	531	Saturne	LES, Dyn. Smagorinsky	6.2M
S25	585	TransAT	LES-WALE	2.5 M
S1	589	Fluent	LES	4.5M
S7	603	CFX	SAS-SST	5.0 M
S15	605	CFX	SAS-SST	2.3M
S13	706	CFX 12.0	SAS-SST	1.1M
S12	712	MODTURC_CLAS	k-epsilon/RNG	0.89M
S29	719	CFX	SAS-SST	1.0M
S28	772	STAR-CCM+	Dynamic Vreman	3.7M

**Table 2 Submissions Ranked by Comparison to Thermocouple Data**

<b>Submission</b>	<b>TC Score</b>	<b>Code</b>	<b>Turbulence</b>	<b>Volumes</b>
S21	36	Nek5000	LES, spectral damping	21M
S16	45	Fluent 12	LES-WALE	7.7M
S8	48	STAR-CCM+/3.06.006	LES-Wale SGS	13.2 M
S4	57	Fluent 6.3.26	LES, Dyn. Smagorinsky	5.8M
S22	72	Star-CCM+	LES	4.4 M
S23	78	CFX	LES-WALE	1.9 M
S5	81	Saturne	LES, Dyn. Smagorinsky	6.2M
S2	82	FLUENT 12.1	LES, Dyn. Smagorinsky	34M
S20	82	FLUENT	LES, Dyn. Smagorinsky	70.5M
S19	83	FLUENT 12.1	SST-kw	11M
S14	88	CABARET	ILES	1.8M
S25	88	TransAT	LES-WALE	2.5 M
S18	93	CFX	DES-SST	2.4M

Submission	TC Score	Code	Turbulence	Volumes
S10	105	Fluent 12	LES-Smagorinsky-Lilly	0.92M
S26	105	FLUENT v12.1	LES - Dynamic KE SGS	7.2 M
S6	110	STAR-CCM+/3.06.006	LES-Wale	9.3 M
S17	121	OpenFOAM 1.6	LES, 1eqn. Dyn. eddy	0.28M
S7	124	CFX	SAS-SST	5.0 M
S11	138	CFX	LES-Wale	3.4M
S1	139	Fluent	LES	4.5M
S24	151	OpenFOAM 1.6	LES, Dyn. Smagorinsky	8 M
S9	164	Advance/FrontFlow/red v4	LES-Smagorinsky	4.1 M
S15	164	CFX	SAS-SST	2.3M
S13	186	CFX 12.0	SAS-SST	1.1M
S27	186	Star-CCM+	V <sup>2</sup> F	0.62 M
S29	197	CFX	SAS-SST	1.0M
S3	201	CFX5 v12	LES, WALE	0.97M
S12	224	MODTURC_CLAS-IST	k-epsilon/RNG	0.89M
S28	232	STAR-CCM+	Dynamic Vreman	3.7M

For those who prefer a metric based on root mean square error, the ranking and scores are very close to those above based upon a mean error magnitude. For a root mean square based metric submissions S3 and S11 swap positions in Table 1, and submissions S19 and S20 swap positions in Table 2. In both instances the scores only differed by one, so these are not significant changes.

### ***Performance on Time Averaged and RMS Velocity Components***

Figures 5 through 8 compare the submissions with the top four results rated by velocity. Quality judgments depend on the goals of an analysis. For many purposes acceptable results for the averaged quantities can be obtained with far less than the 70 million volumes used in the LES analysis of submission 20.

Note that the submission with the smallest number of volumes (S4, 5.8M volumes), fails to capture the shape of the time averaged U profile at  $x=4.6D$ ,  $z=0$ . While results from the other three LES calculations retain two slight maximums off-center, S4 has a maximum at or near the pipe centerline.

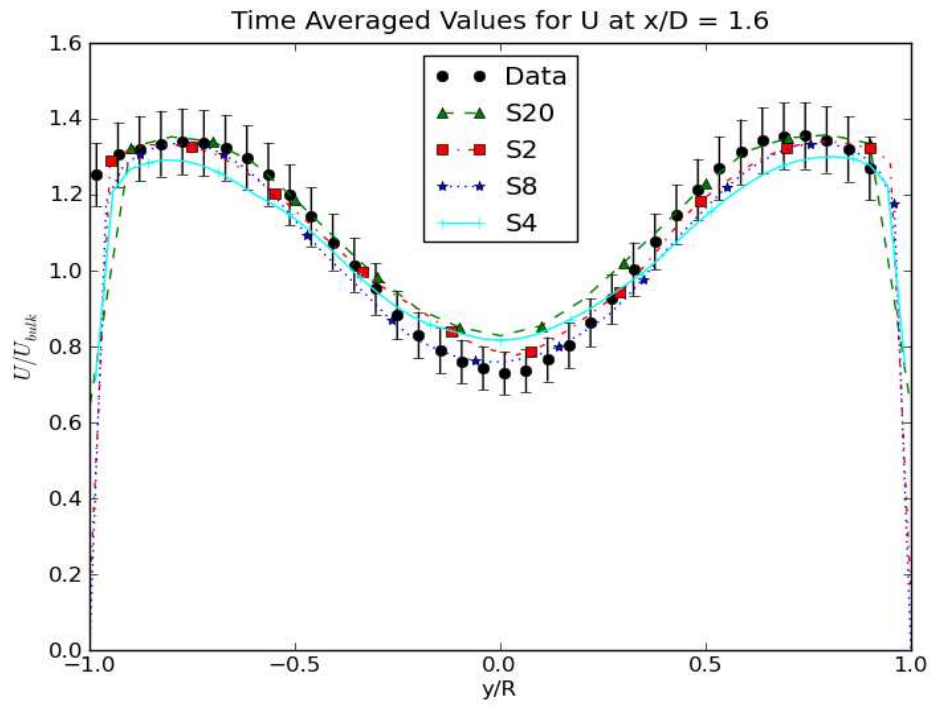


Figure 6: Time Averaged U at  $x = 1.6D$ ,  $z = 0$

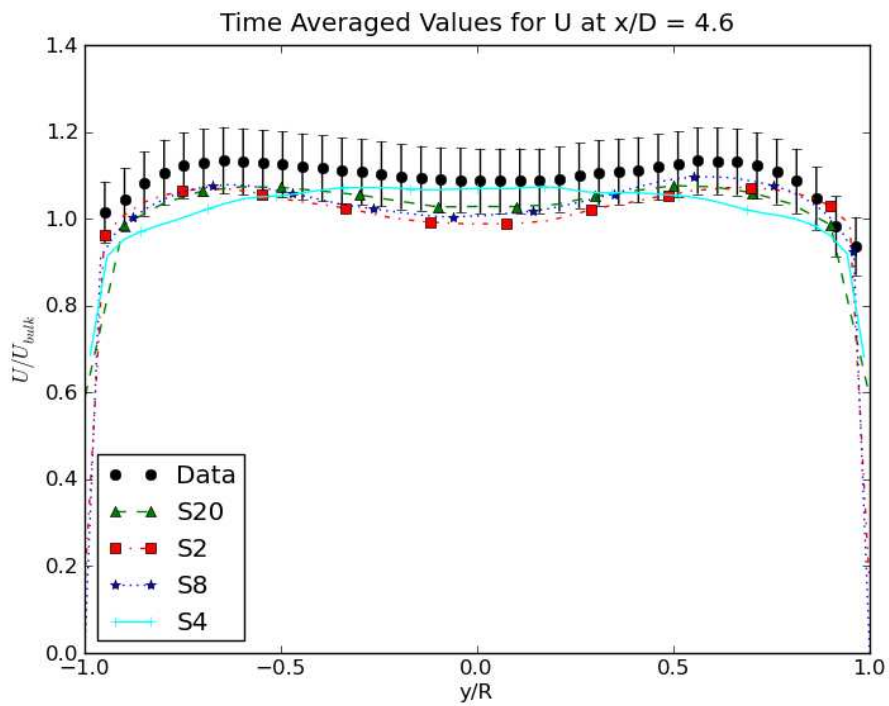


Figure 5: Time Averaged U at  $x = 4.6D$ ,  $z = 0$



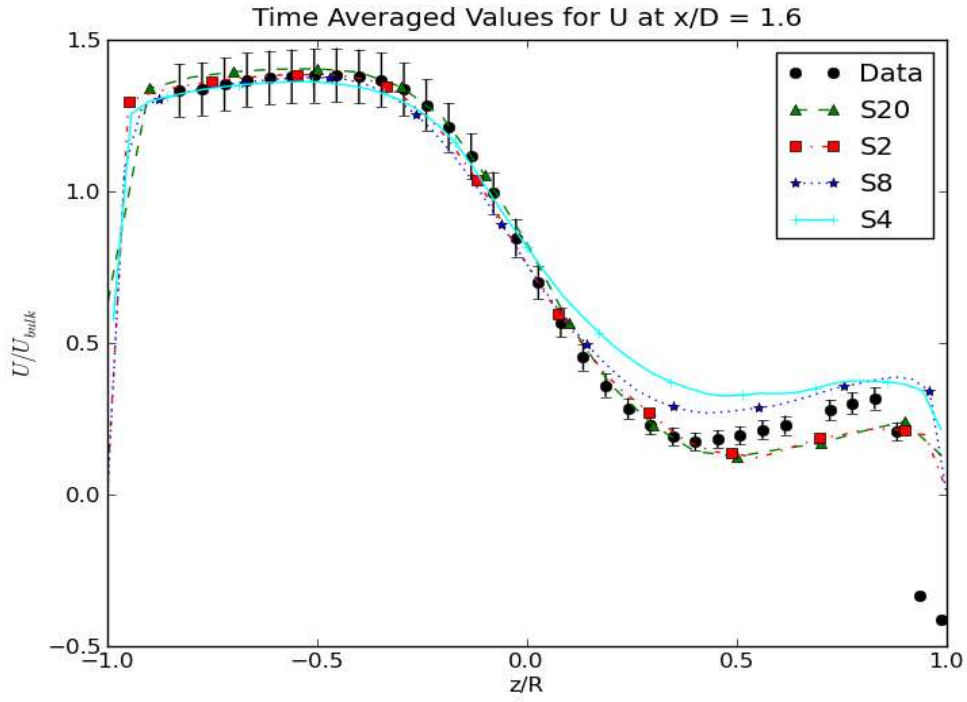


Figure 7: Time Averaged U at  $x = 1.6D$ ,  $y = 0$

§

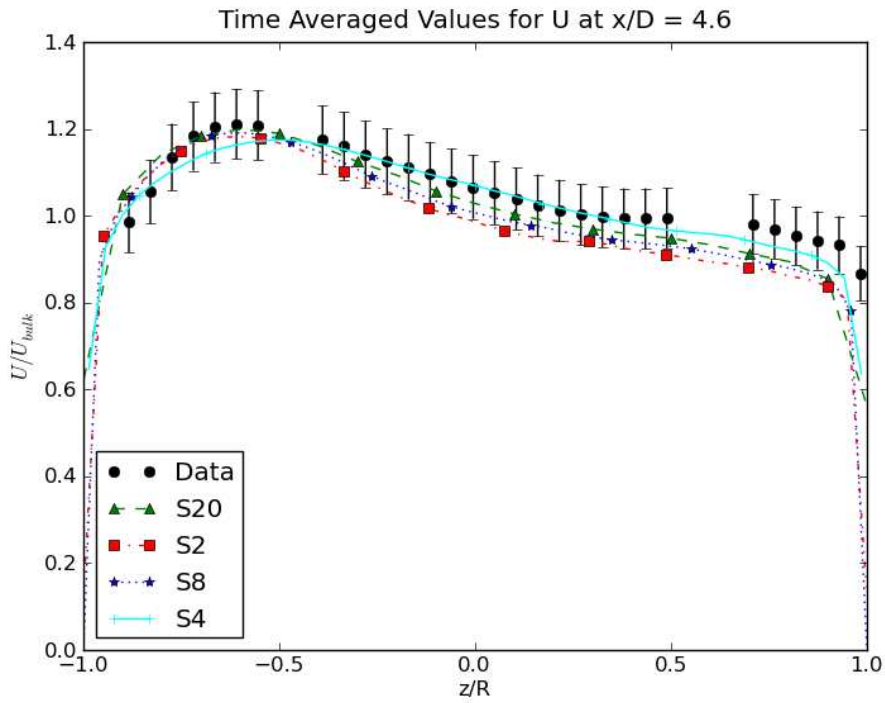
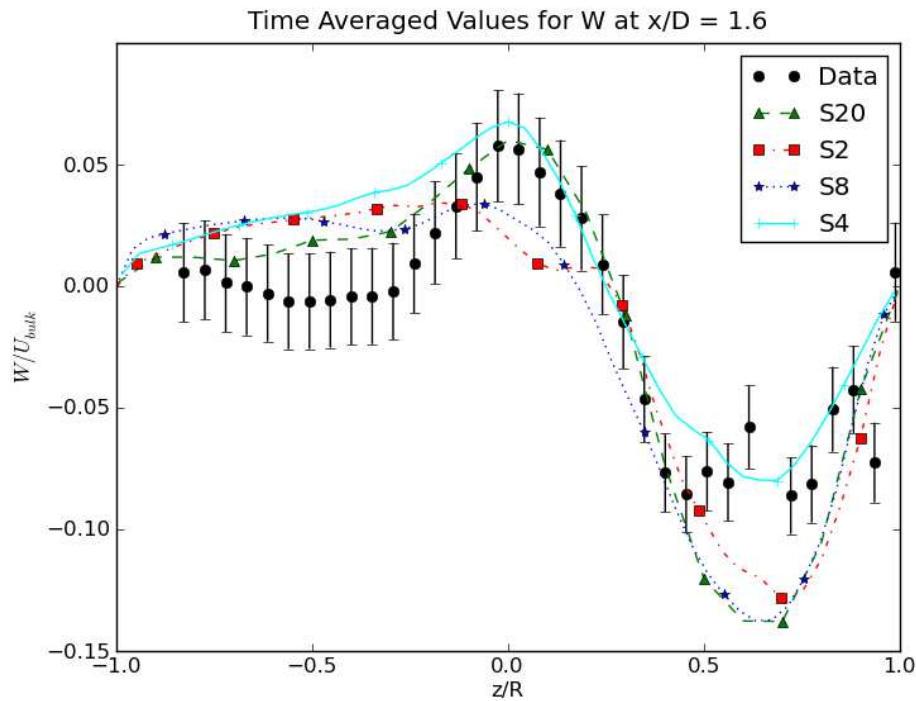


Figure 8: Time Averaged U for  $x = 4.6D$ ,  $y = 0$

We've already seen in Figure 4 that results for time averaged  $V$  are poor, due to the symmetry about the  $y = 0$  plane. Figure 9 shows that results are not as close for time averaged  $W$  as already seen for time averaged  $U$ . However, the basic shape of the curve is preserved by all calculations.



**Figure 9: Time Averaged  $W$  for  $x = 1.6D$ ,  $y=0$**

Compare the quality of results for the RMS value of  $v$  in Figure 10 to those for time averaged  $V$  in Figure 4. For these LES calculations it is normal to have reasonable predictions of RMS velocity fluctuations even when predictions of time averaged velocities are relatively poor.

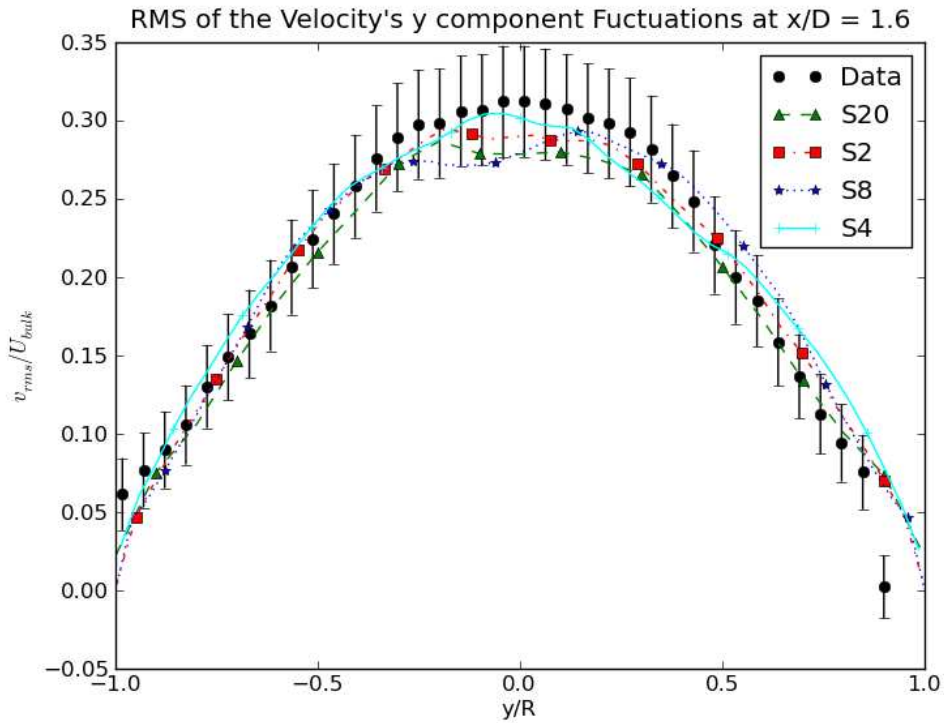


**Figure 10: Time averaged RMS  $v$  for  $x = 1.6D$ .  $z = 0$**

The following six figures compare results from the best of the LES calculations using a dynamic Smagorinsky model to those from the best of the Scale-Adaptive Simulation approach with the Shear Stress Transport model (SAS-SST) along with those from use of a Detached Eddy Simulation (DES) model with SST, and a Very Large-Eddy Simulation (VLES) with an SST- $k\omega$  turbulence model. They correspond to Figures 5 through 10 for the LES runs.

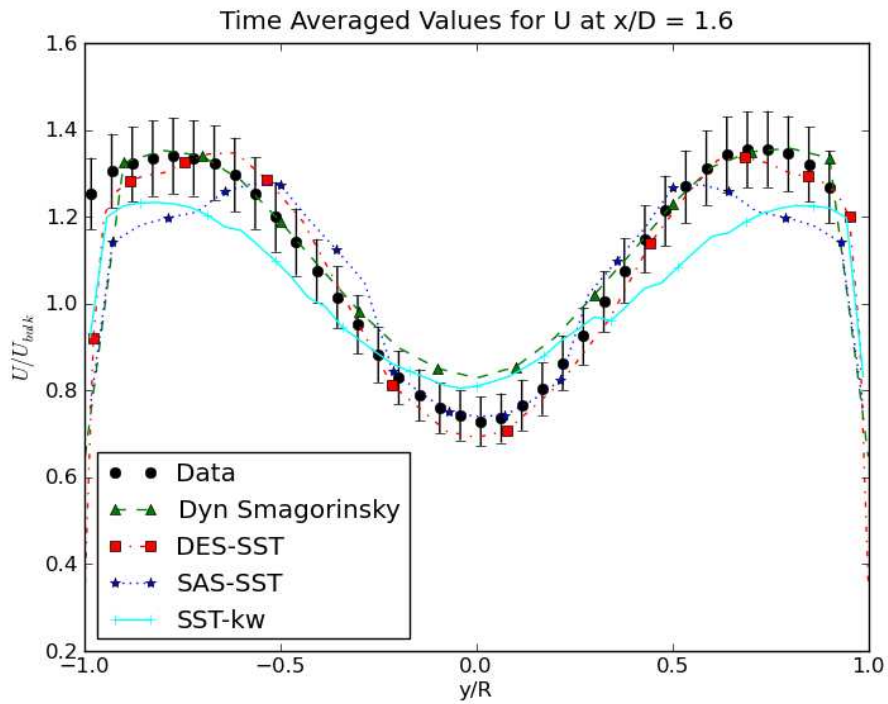


Figure 11: Comparison of Time Averaged U at  $x = 1.6D$ ,  $z=0$

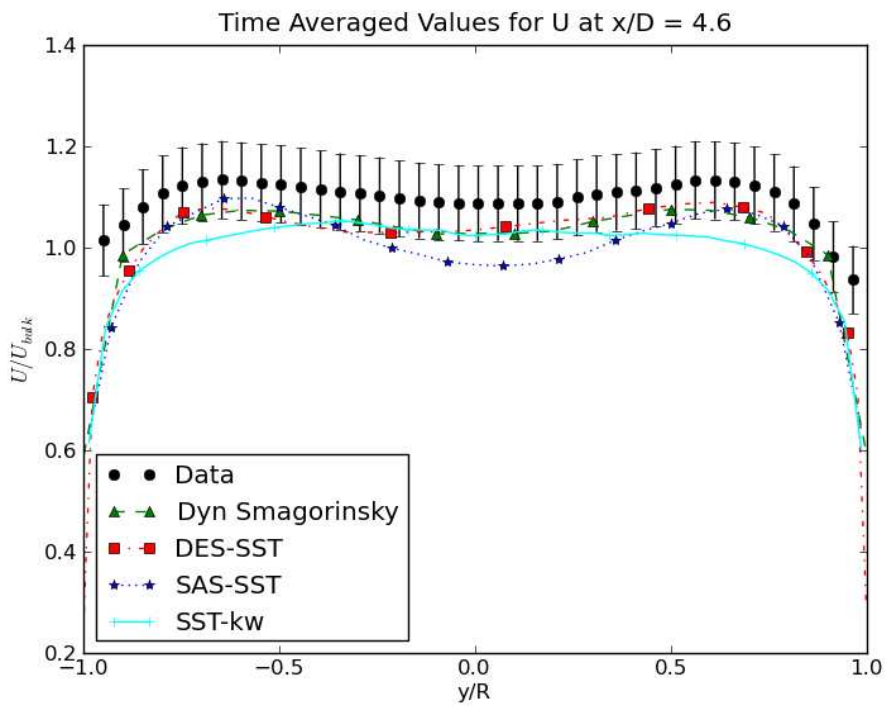


Figure 12: Comparison of Time Averaged U at  $x = 4.6D$ ,  $z=0$

For Figure 11 the SAS-SST results have maximums that are significantly closer to the centerline than experimental or other CFD results. The SST- $k\omega$  analysis has significantly lower difference between magnitudes of maximums and the central minimum. The DES-SST does exceptionally well given the relatively low number of computational volumes (2.4M). For Figure 12 ( $x=4.6D$ ,  $z=0$ ) the SST- $k\omega$  analysis has lost the double maximums, and SAS-SST has a larger difference between the maximums and the central minimum.

SAS-SST also shows distortions in time averaged U profiles along the z direction. Values are lower than they should be below the centerline and significantly higher than they should be above the centerline at  $x = 1.6D$  (Figure 13). At  $x = 4.6D$  the values aren't too out of line with data, but the shape of the curve is significantly different, retaining a central minimum (Figure 14).

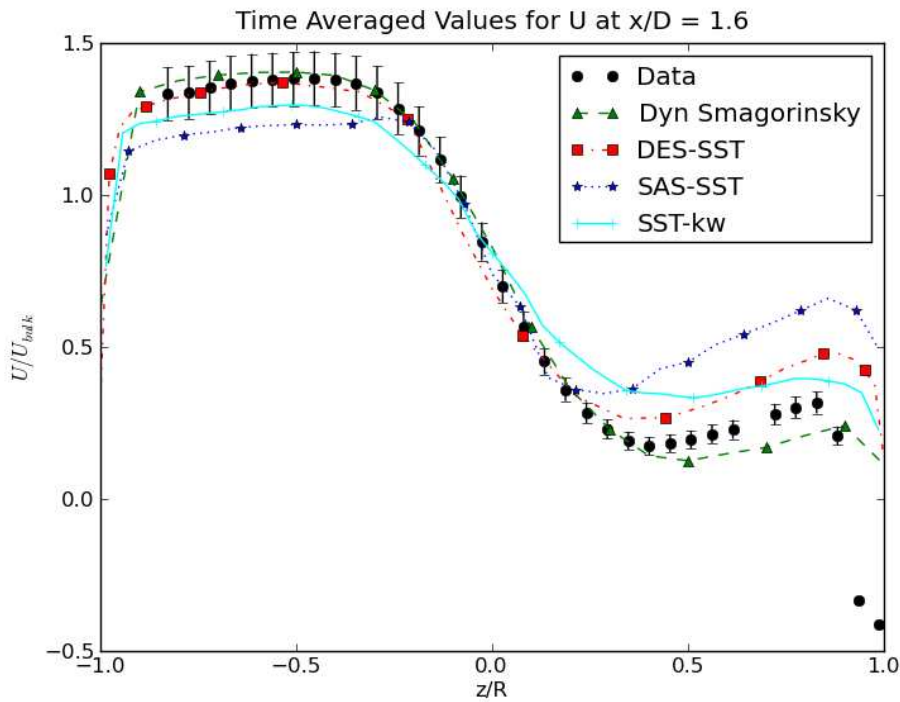


Figure 13: Comparison of Time Averaged U at  $x=1.6D$ ,  $y=0$

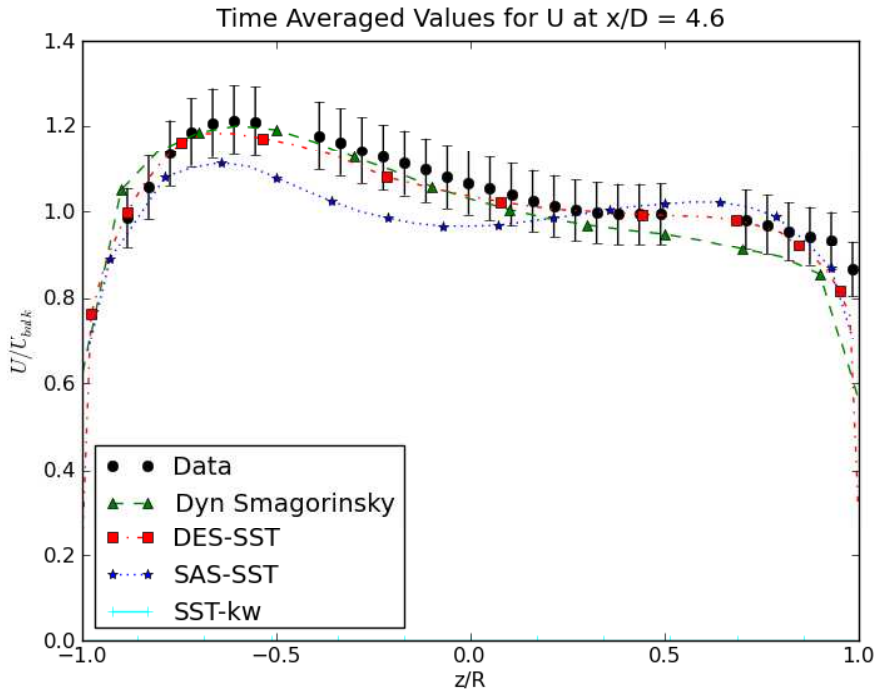


Figure 14: Comparison of Time Averaged U at  $x = 4.6D$ ,  $y=0$

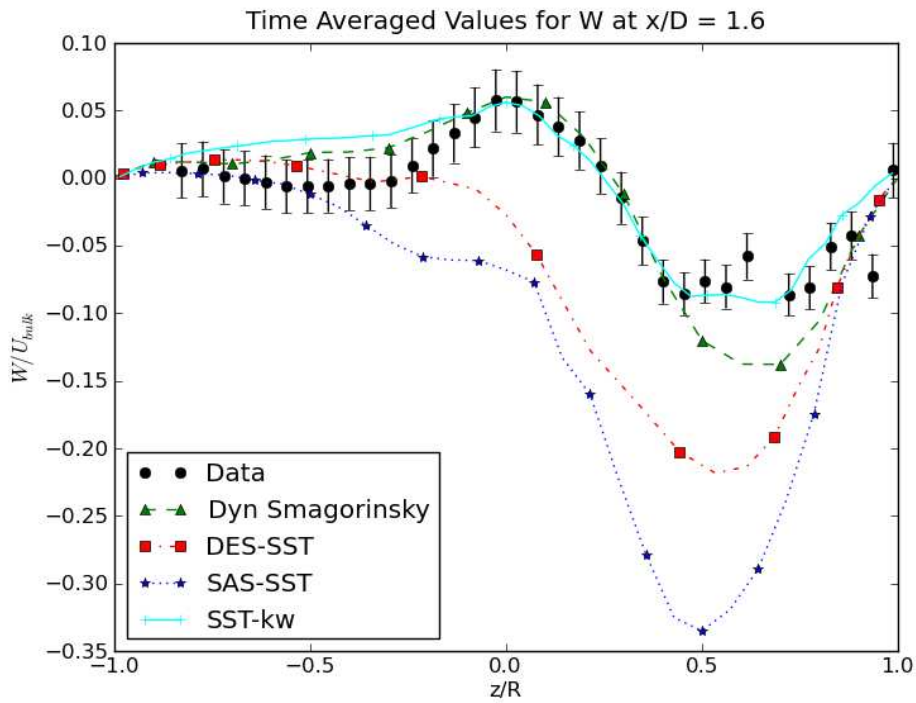
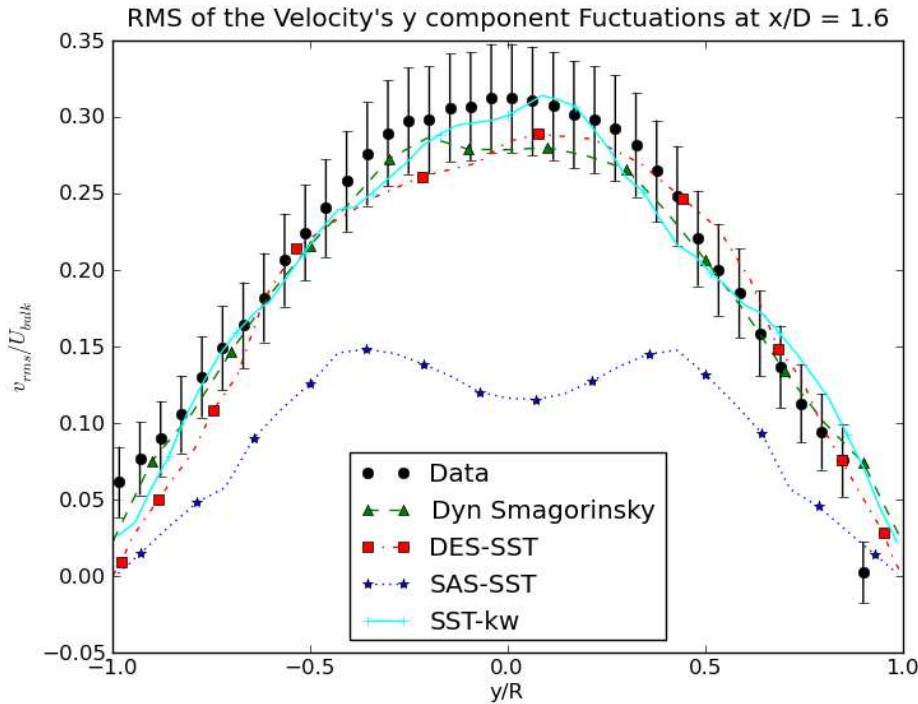


Figure 15: Comparison of Time Averaged W at  $x = 1.6D$ ,  $y=0$



**Figure 16: Comparison of RMS Fluctuations in V for  $x = 1.6$ ,  $z = 0$**

Problems with use of CFX and the SAS-SST turbulence model for this particular flow pattern suggest a need for better guidelines for use of this model. Given the results for DES-SST with CFX, the guidelines might simply recommend use of the DES rather than SAS option for some range of flow conditions. However, specific conclusions will require careful consideration of input details for submissions S7 and S18 not available in documentation requested for this benchmark exercise.

### ***Performance on Time Averaged and RMS Temperature***

Some significant shifts occur in ranking between Table 1 and Table 2. However, much of that reflects the very similar behavior in results for the flow field over a wide range of submissions. Figures 17 through 20 show that predictions of the time averaged component of velocity along the pipe are very close for the runs that are highest rank on velocity predictions (S20 and S2) and those with the highest rank on temperature predictions (S16 and S21).

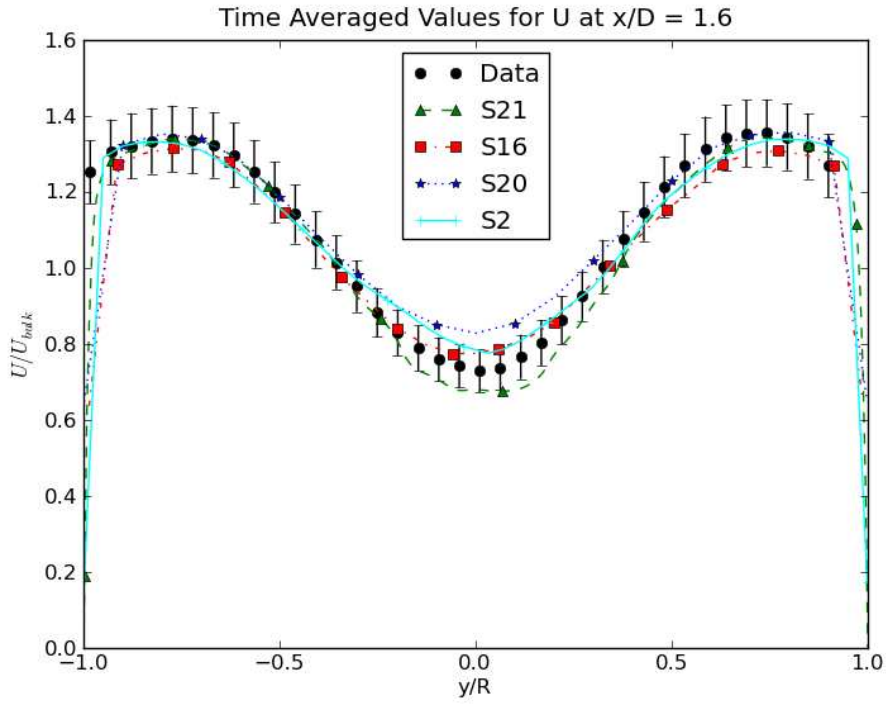


Figure 17: Time Averaged U at  $x=1.6D$ ,  $z=0$

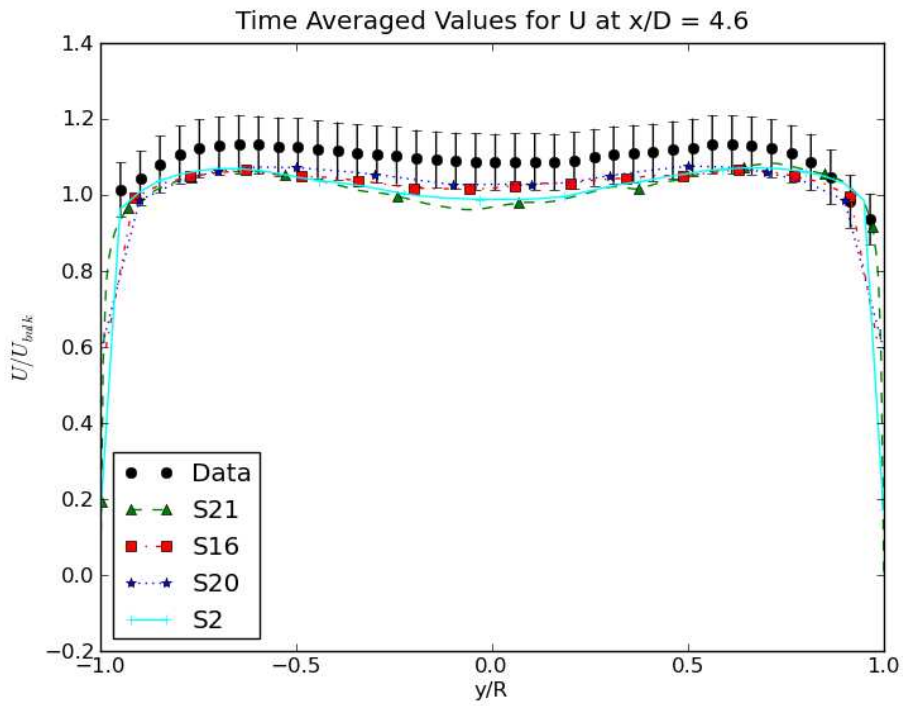


Figure 18: Time Averaged U at  $x = 4.6D$ ,  $z = 0$



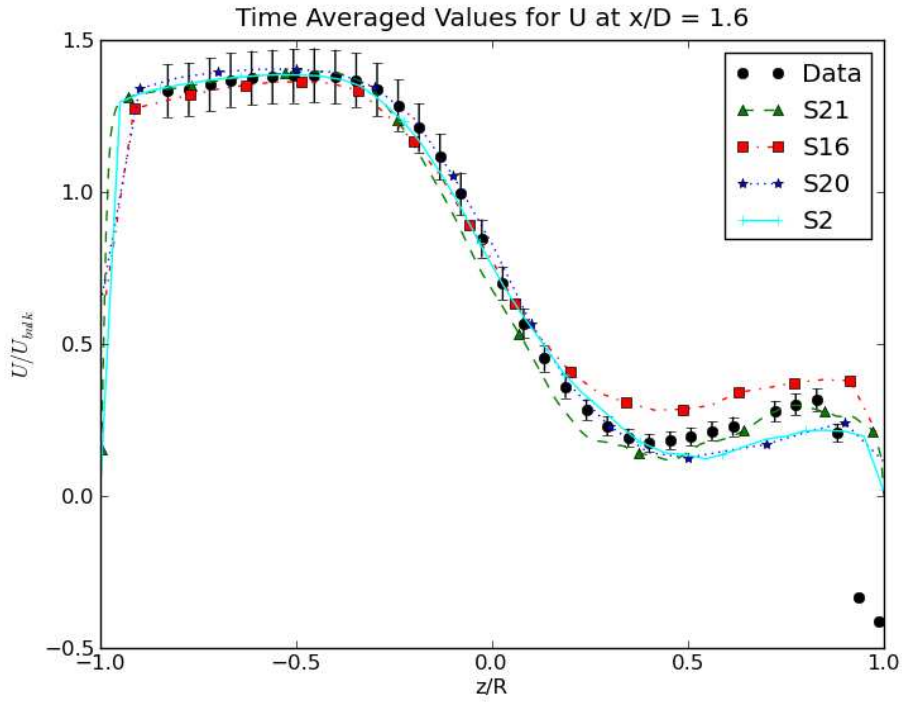


Figure 19: Time Averaged U at  $x = 1.6, y = 0$

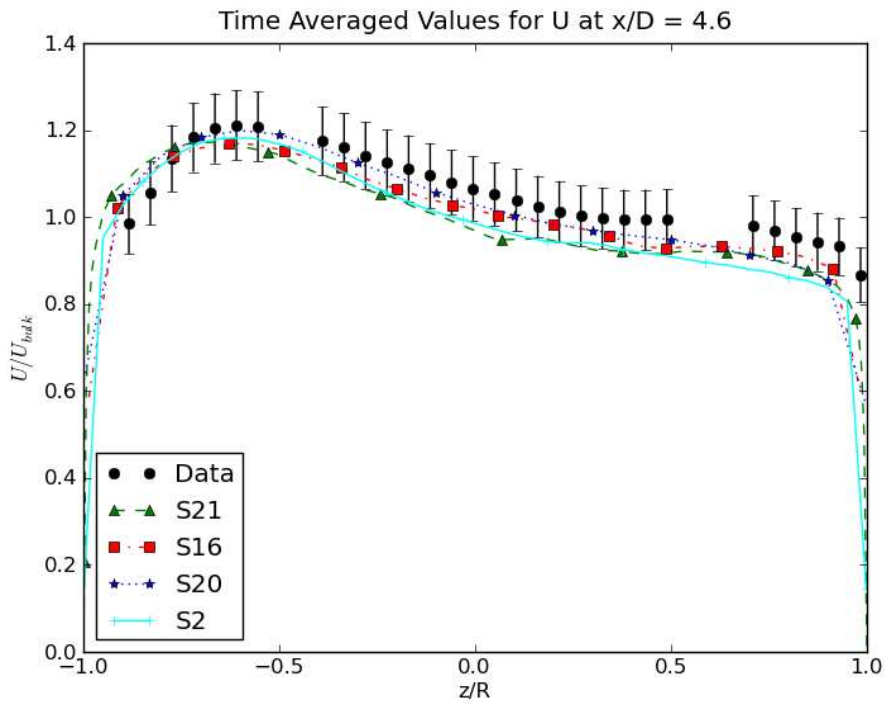
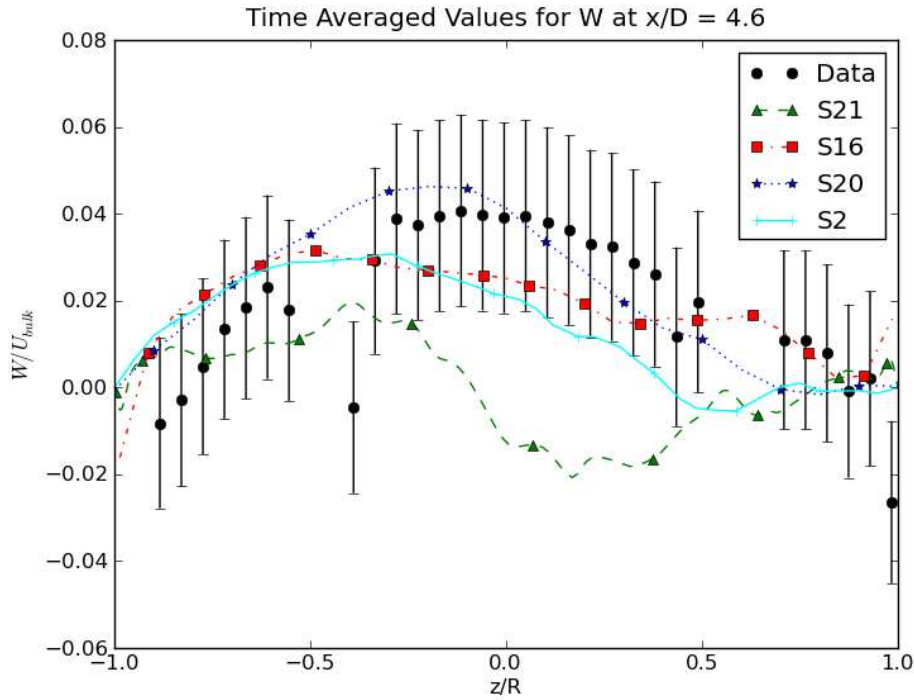


Figure 20: Time Averaged U at  $x=4.6D, y=0$

Lower ranking on comparison with velocity data for submission 21 (a spectral element method) can be attributed to systematically poorer matches to the time averaged z component of velocity further downstream of the tee junction (e.g. Figure 21). Lower ranking of submission 16 in Table 1 is primarily a result of slightly poorer comparison on RMS velocity fluctuations.



**Figure 21 Time Averaged W at  $x = 4.6D$ ,  $y = 0$**

Temperatures were reported in a non-dimensional form.  $T^*$  is the actual temperature minus the cold flow inlet temperature, divided by the difference between hot and cold inlet temperatures. For this benchmark case the hot inflow temperature is  $36^\circ\text{C}$  and the cold is  $19^\circ\text{C}$ .

Figures 22 through 25 give experimental and calculated values for runs S21, S16, S20, and S2. RMS fluctuations in  $T^*$  are provided in Figures 26 through 29.

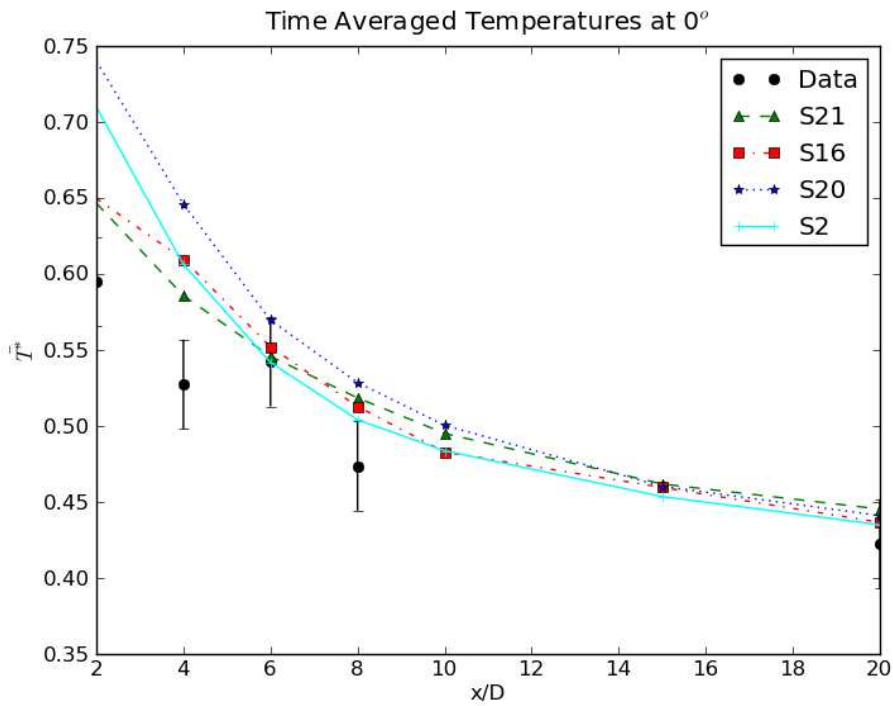


Figure 22: Time Averaged Temperatures at Top of Pipe

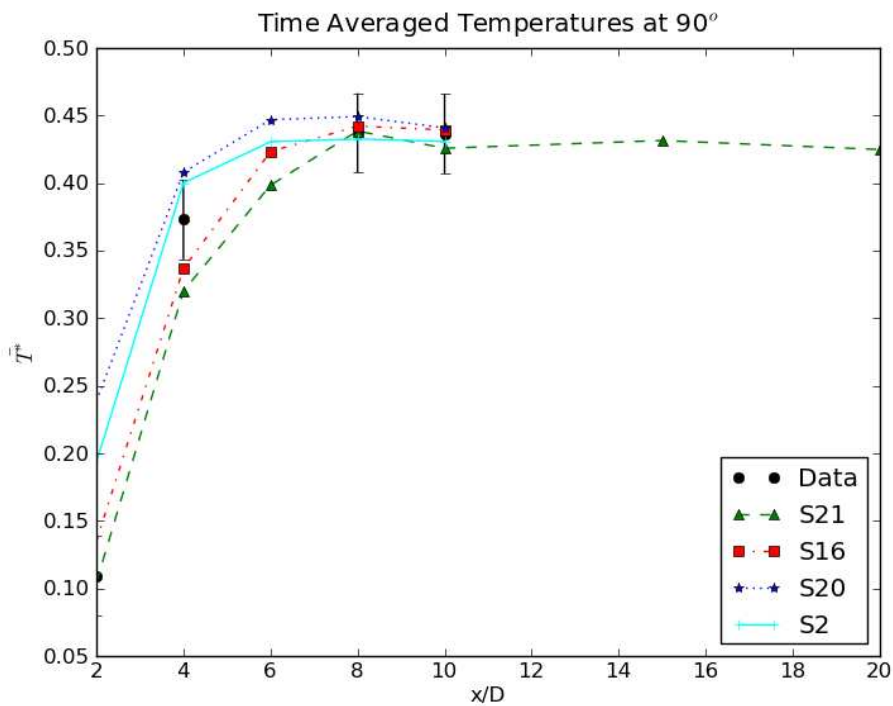


Figure 23 Time Averaged Temperature at  $90^\circ$

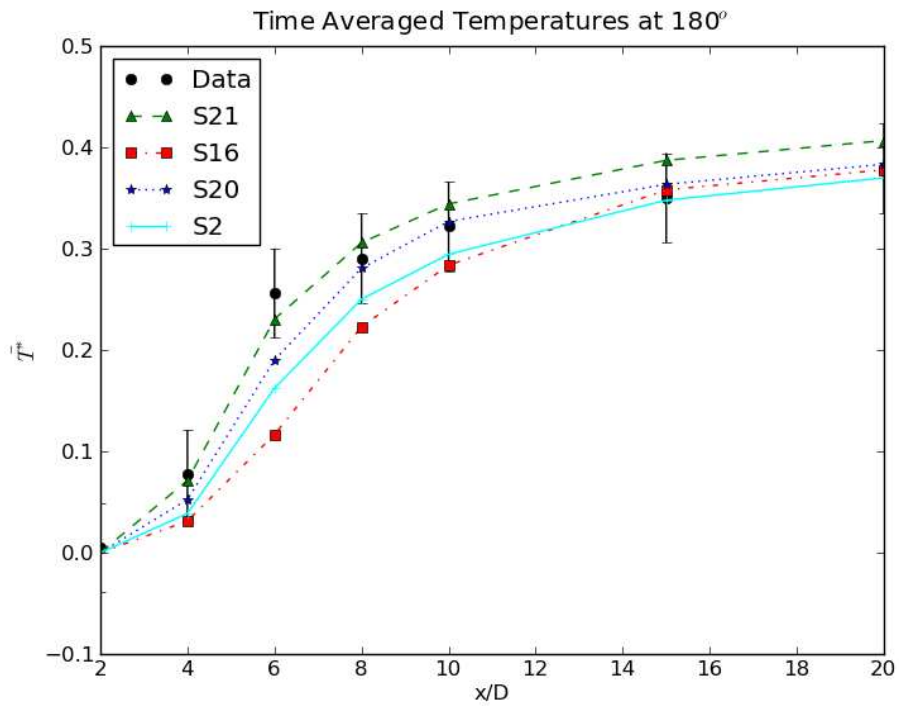


Figure 24 Time Averaged Temperature at Bottom of Pipe

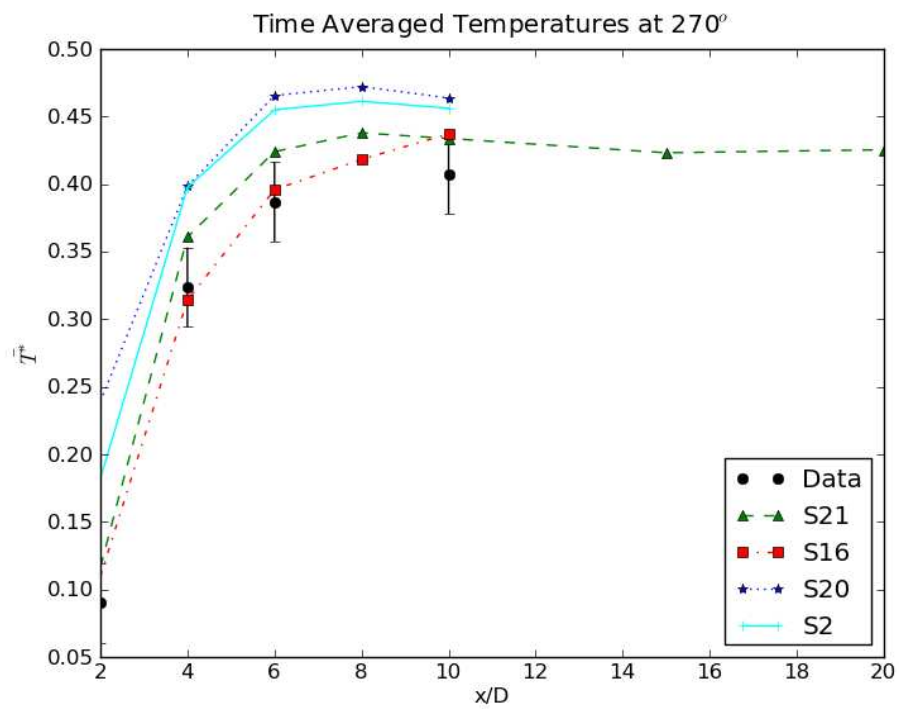


Figure 25: Time Averaged Temperatures at 270°

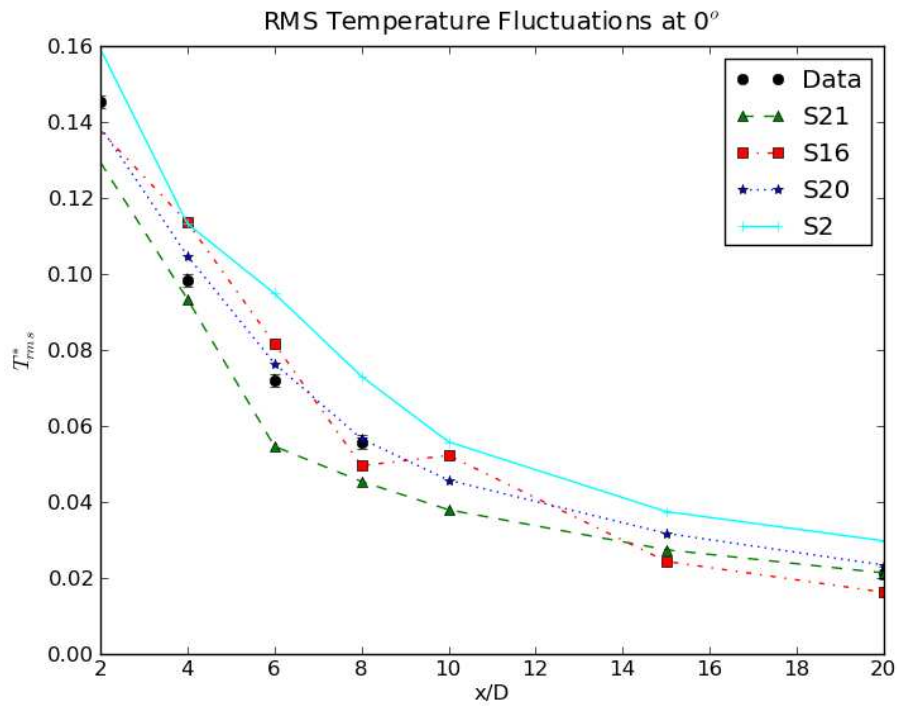


Figure 26: RMS Temperature Fluctuations at Top of Pipe

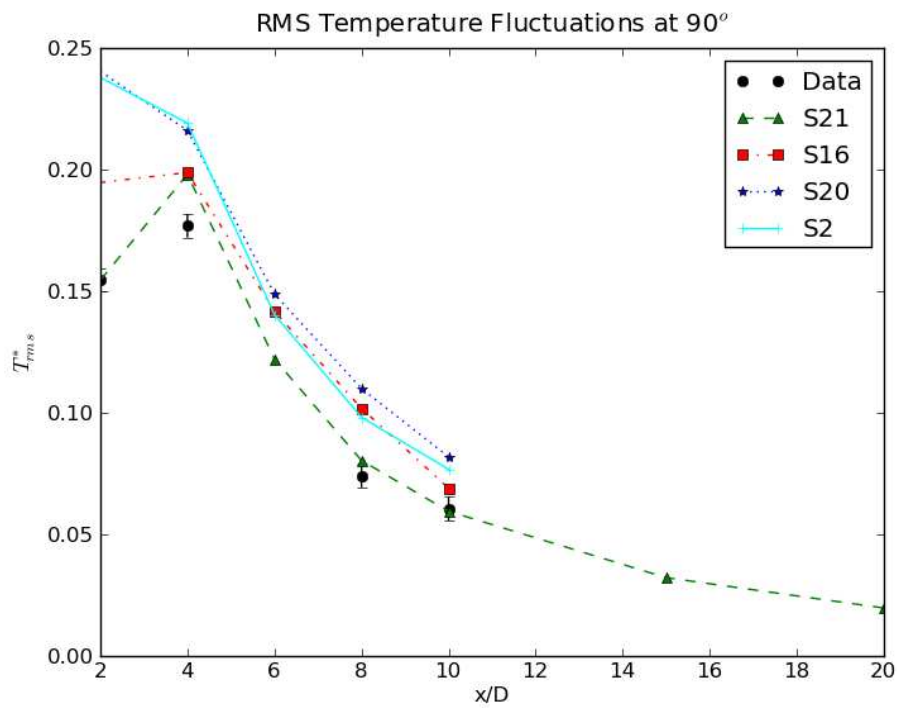


Figure 27: RMS Temperature Fluctuations at  $90^\circ$

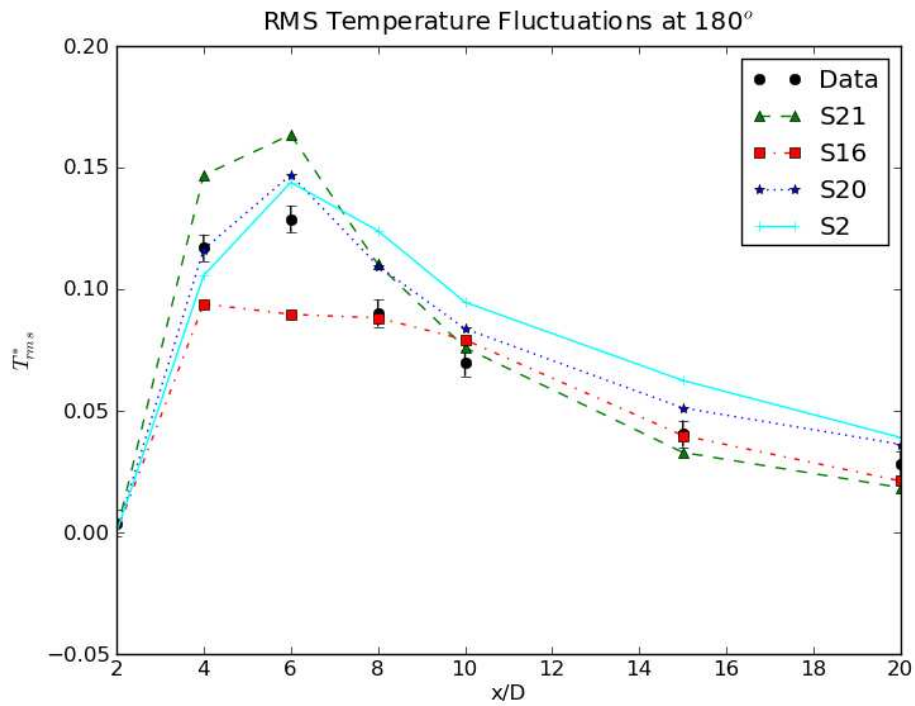


Figure 28: RMS Temperature Fluctuations at Bottom of Pipe

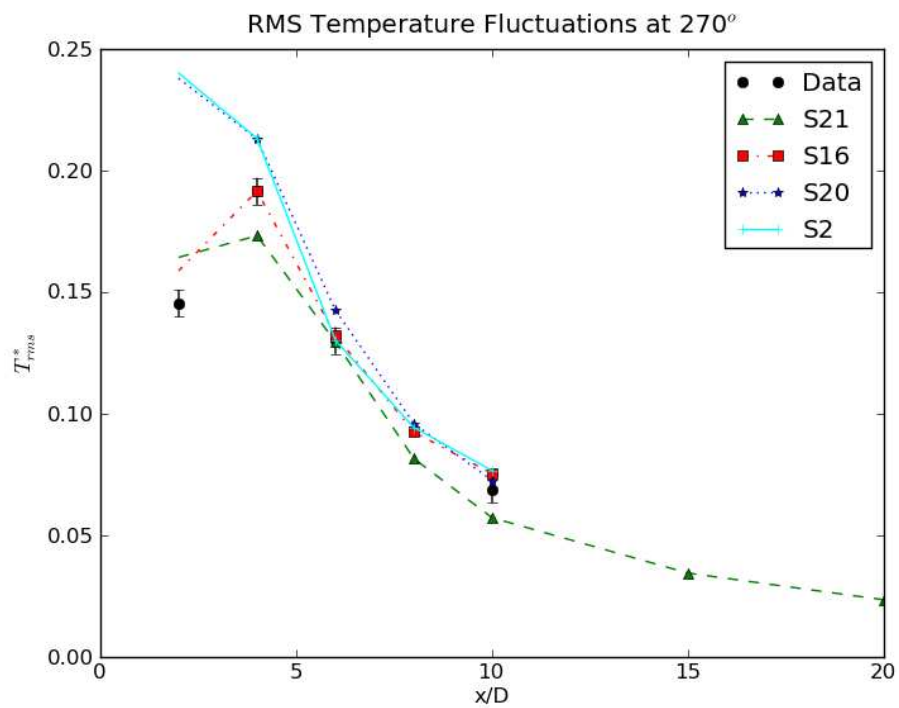


Figure 29: RMS Temperature Fluctuations at 270°

Although S2 and S20 do well for the bottom thermocouple results, they have mixed more of the hot stream to other thermocouples nearer to the tee junction, explaining their lower rating for temperature results.

### **Fourier Analysis**

The primary goal of Fourier analysis is to check for simulation of periodic low frequency flow oscillations. A secondary goal is to compare the turbulence spectrum predicted by LES with that seen in data. Comparison of calculations to experimental data or other calculations is a little tricky. For a meaningful comparison of amplitudes from the discrete Fourier transform, all data sets being compared should have the same time duration and same sampling frequency. Because amplitudes generally drop rapidly with frequency, this analysis does not attempt to re-sample data sets at a set frequency. This approximation does not have a significant effect on the primary goal of the analysis.

Comparison of CFD results was much less automated than those presented in previous sections due to time requirements to assemble a good set of tools for spectral analysis. Twenty-nine plot sets were produced comparing transforms of each set of transient CFD results to the experimental data. A long period of visual inspection followed, where notes were made of data locations (e.g. thermocouple 2D90, v on centerline at  $x=1.6D$ ) with spectral peaks in both CFD and experimental data near 3.5 Hz. Co-location of peaks does not imply a match in the height of the peaks. Finally the number of thermocouples with the match was totaled for each CFD calculation, and the same operation was performed for all available transient PIV information.

Table 3 lists all submissions with more than 5 matches to peaks in PIV spectra near 3.5 Hz.

**Table 3 Number of Matches for PIV Peaks**

Label	PIV Count	Code	Turbulence	Duration	Total nodes
S4	27	Fluent 6.3.26	LES, Dynamic Smagorinsky	15 s	5.8M
S20	23	FLUENT	LES-Dynamic-Smagorinsky	23 s	70.5M
S8	17	STAR-CCM+/3.06.006	LES-Wale SGS	28 s	13.2M
S18	16	CFX	DES-SST	13 s	2.4M
S26	14	FLUENT v12.1	LES - Dynamic Kinetic Energy SGS Model	18 s	7.2 M
S6	14	STAR-CCM+/3.06.006	LES-Wale	10 s	9.3 M
S1	13	Fluent	LES	5 s	4.5M
S17	13	OpenFOAM 1.6	LES, 1eqn. Dynamic eddy	20 s	0.28M
S19	12	FLUENT 12.1	SST-kw	10 s	11M
S27	12	STAR-CCM+	V <sup>2</sup> F	5 s	0.62 M

Label	PIV Count	Code	Turbulence	Duration	Total nodes
S2	11	Fluent 12	LES, Dynamic Smagorinsky	20 s	34M
S10	9	Fluent 12	LES-Smagorinsky-Lilly	14 s	0.92M
S11	9	CFX	LES-Wale	6.9s	3.4M
S24	9	OpenFOAM 1.6	LES-Dynamic-Smagorinsky	5 s	8 M
S25	9	TransAT	LES-WALE	5.5 s	2.5 M
S16	8	Fluent 12	LES-WALE	5.5 s	7.7M
S21	8	Nek5000	LES, spectral damping	5.9 s	21M
S5	8	Saturne	LES, Dynamic Smagorinsky	5 s	6.2M
S22	7	Star-CCM+	LES	6.2 s	4.4 M

Although only minimal signs are seen of a peak in the temperature spectrum for the CFD results around 3.5 Hz, a significant number of peaks are seen there in the frequency spectra for U and V velocity components. This indicates that some reproduction of the physical flow oscillations is present in CFD results.

The count of matching peaks is only a partial measure of success in simulating flow oscillations; nearly all submissions in Table 3 had peaks in the spectrum for the y component of velocity ( $v$ ) along the centerline. Submission 5 is near the bottom of the list, but did fairly well matching the experiment at these locations (see Figure 30). However, other details of the oscillations are different in this LES calculation from the experiment. Spectral peaks seen halfway from the center to the wall along a horizontal line are missing from the calculation (see Figure 31). However, the calculation has spectral peaks halfway from the center to the wall along a vertical line that are not present in the experiment (see Figure 32). It would be interesting to see how sensitive the oscillation mode is to relatively minor changes in nodalization or boundary conditions.



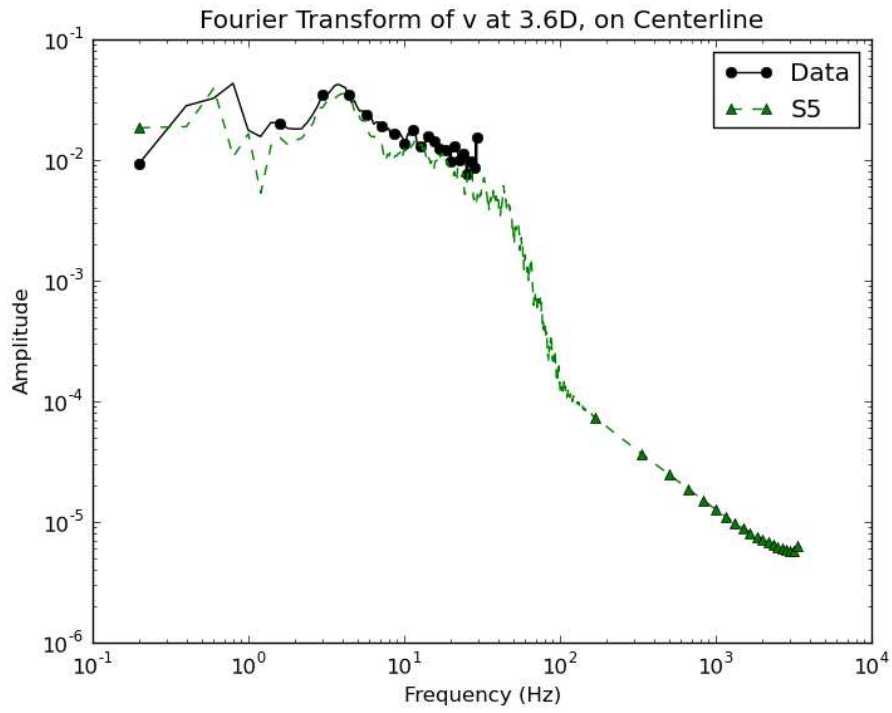


Figure 30: Fourier Amplitudes for S5 and Data,  $v$  at  $x = 3.6D$ ,  $y=0$ ,  $z=0$ .

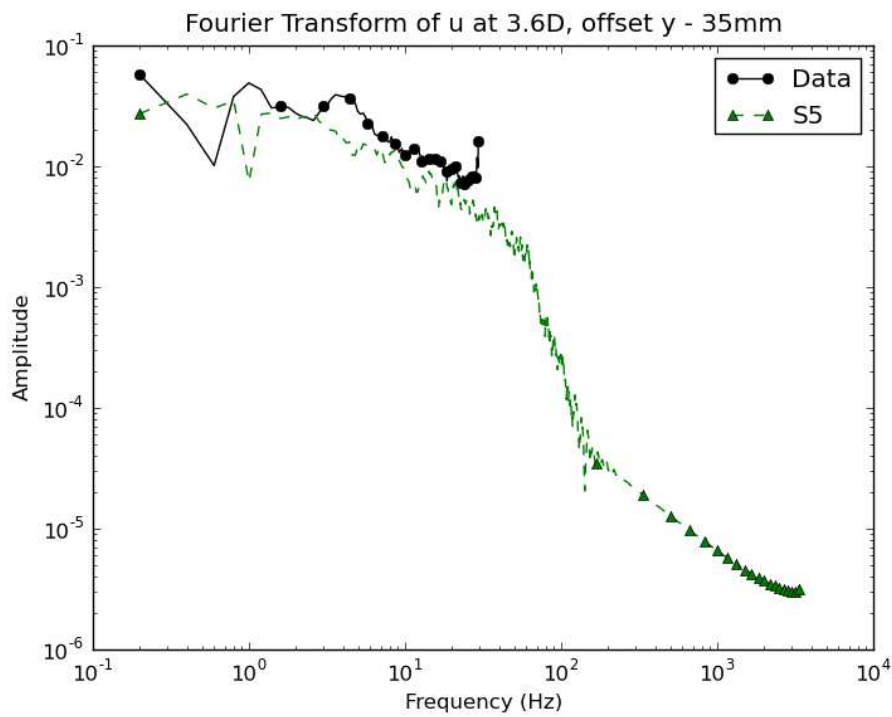
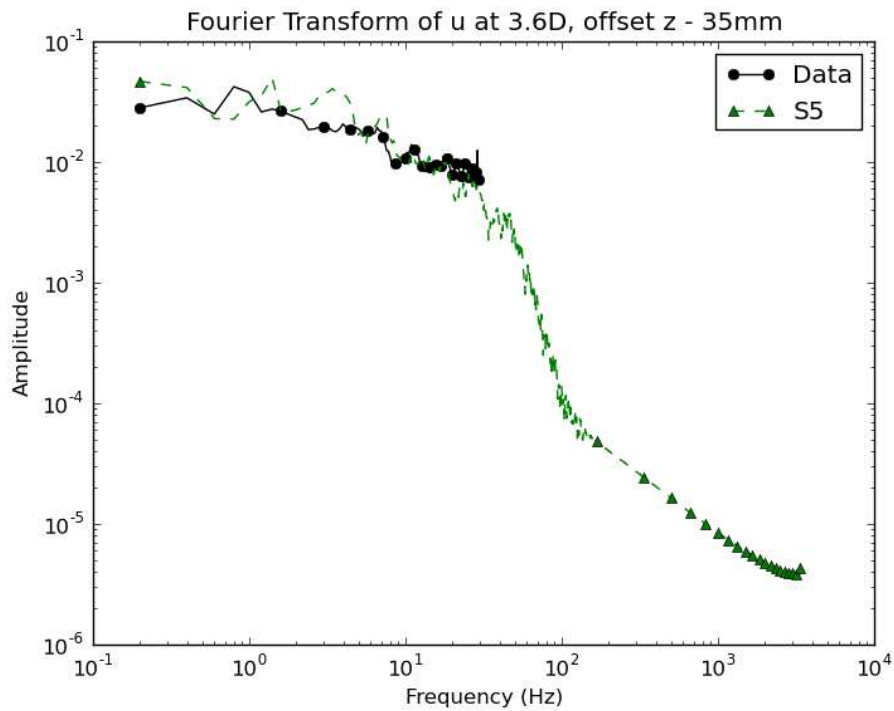


Figure 31: Fourier Amplitudes for S5 and Data,  $u$  at  $x=3.6D$ ,  $y=-35\text{mm}$ ,  $z=0$



**Figure 32: Fourier Amplitudes for S5 and Data, u at  $x=3.6D$ ,  $y=0$ ,  $z=-35\text{mm}$ .**

Submission 4 has a similar number of volumes and the same choice of turbulence model as Submission 5, but does a significantly better job capturing the periodic flow oscillations. The match of spectra for  $v$  on the centerline (Figure 33) is of similar quality to Submission 5, oscillations in the  $z=0$  plane are at least partially captured (Figure 34), and spurious oscillations in the  $y=0$  plane are absent (Figure 35). Differences in experimental data spectra presented for the two submissions are due to different sample durations for the experimental data.

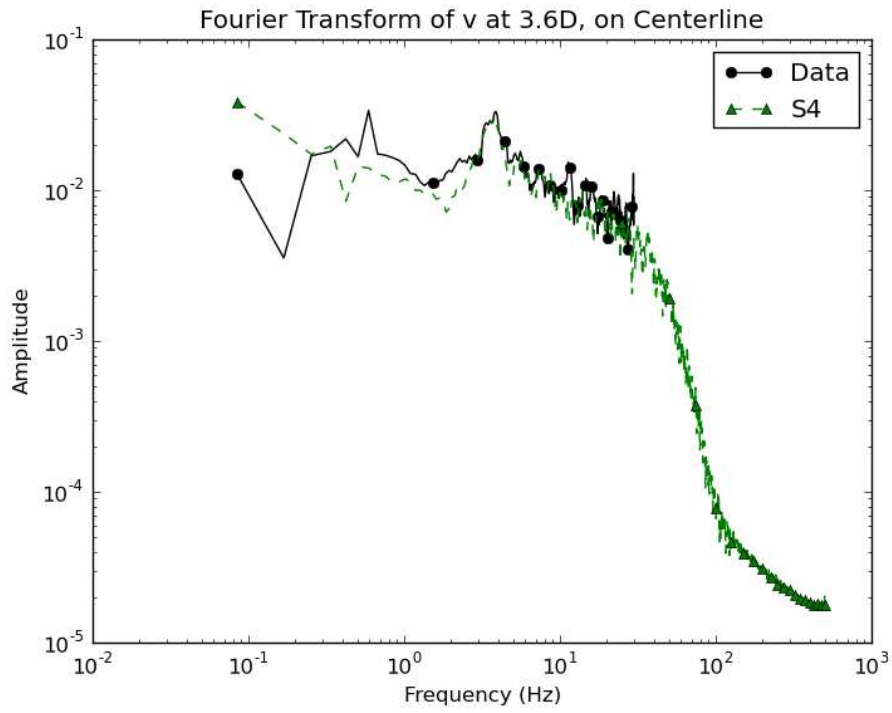


Figure 33: Fourier Amplitudes for S4 and Data,  $v$  at  $x=3.6D$ ,  $y=0$ ,  $z=0$

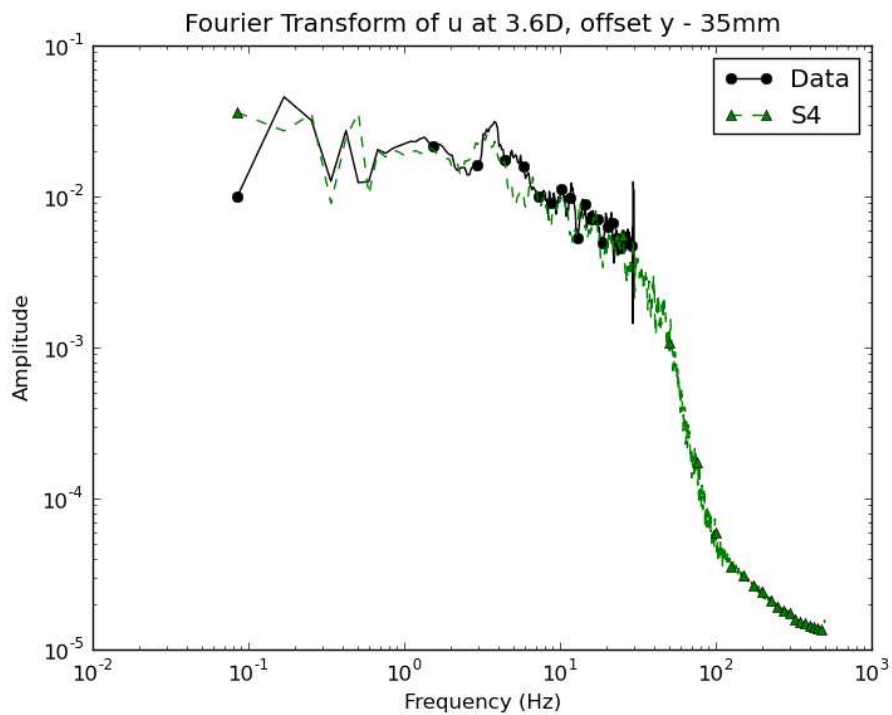
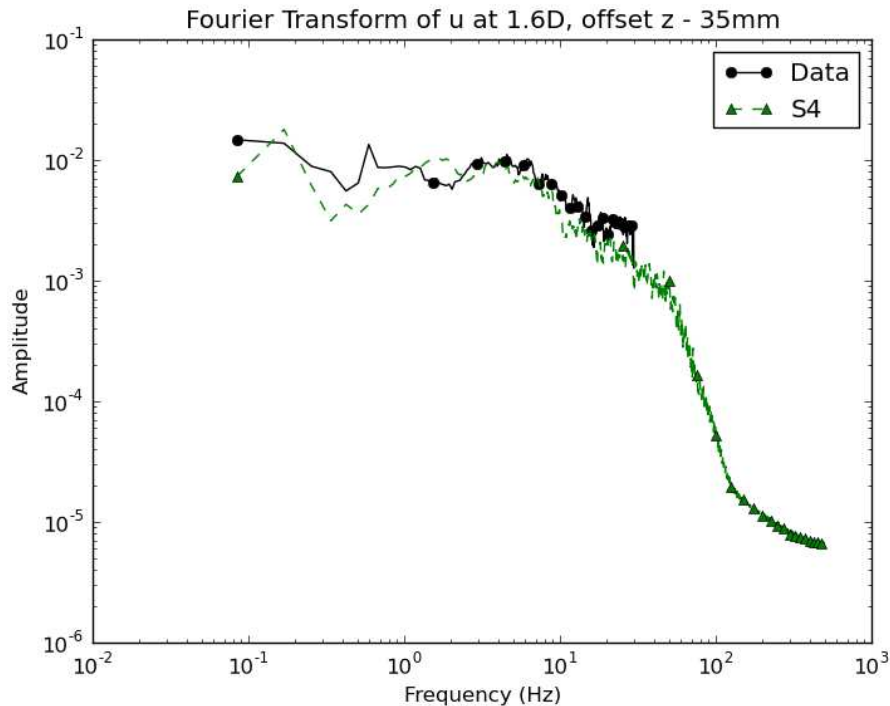


Figure 34: Fourier Amplitudes for S4 and Data,  $u$  at  $x=3.6D$ ,  $y=-35\text{mm}$ ,  $z=0$



**Figure 35: Fourier Amplitudes for S4 and Data,  $u$  at  $x=3.6D$ ,  $y=0$ ,  $z=-35\text{mm}$ .**

Nothing has been said about Fourier spectra of transient temperature results thus far due to the relatively weak peaks. However, there is one phenomenon related to overall shape of the spectra worth noting. At frequencies above about 10 Hz, LES calculations with higher numbers of volumes contain a frequency range with a flatter slope than the data (Figure 36). Note that Submission 21 uses spectral elements rather than a standard CFD approach, but shows the same trends as two finite volume calculations. For smaller numbers of total volumes the spectra for the CFD results line up well with data until frequencies at which turbulence is not being well resolved and amplitudes drop rapidly (Figure 37).

PIV data has not been provided very near to the thermocouples. Figure 38 provides the discrete Fourier transform of  $u$  at a nearby location. The results from 70 million volumes, 6 million volumes, and experimental data overlay well up to the cutoff of experimental results. However, discrete Fourier transforms of CFD results a millimeter from the wall show trends similar to those seen in Figure 36 and Figure 37, although not as pronounced. Distortion of the basic turbulence spectrum near the wall is a possible cause of discrepancies above 10 Hz.

Unfortunately, we did not collect details on approaches used for evaluation of the energy conservation equation and modeling of turbulent thermal conductivity. There could be a mesh dependency in a common approach to modeling energy transport, or there could be a systematic difference in modeling approaches between those using 5-7 million volumes and those using more than 20 million. One argument for a mesh dependent effect is seen in Figure 39. The temperature spectrum for a STAR-CCM+ calculation using LES-WALE and approximately 13 million volumes falls between results presented in Figures 36 and 37.

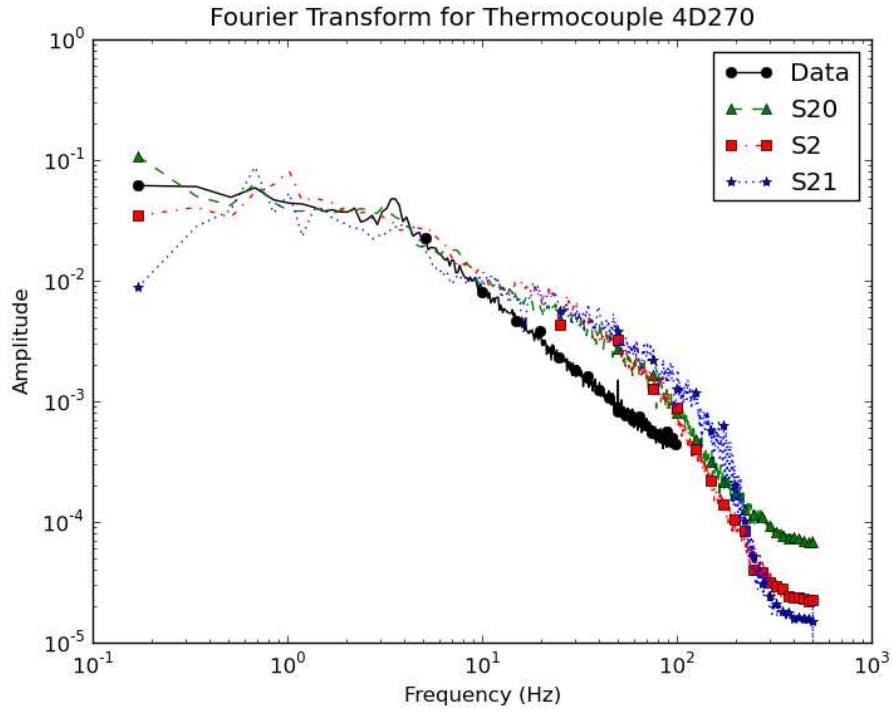


**Figure 36: Flutter Spectrum with more Highly Nodalized LES Submissions**

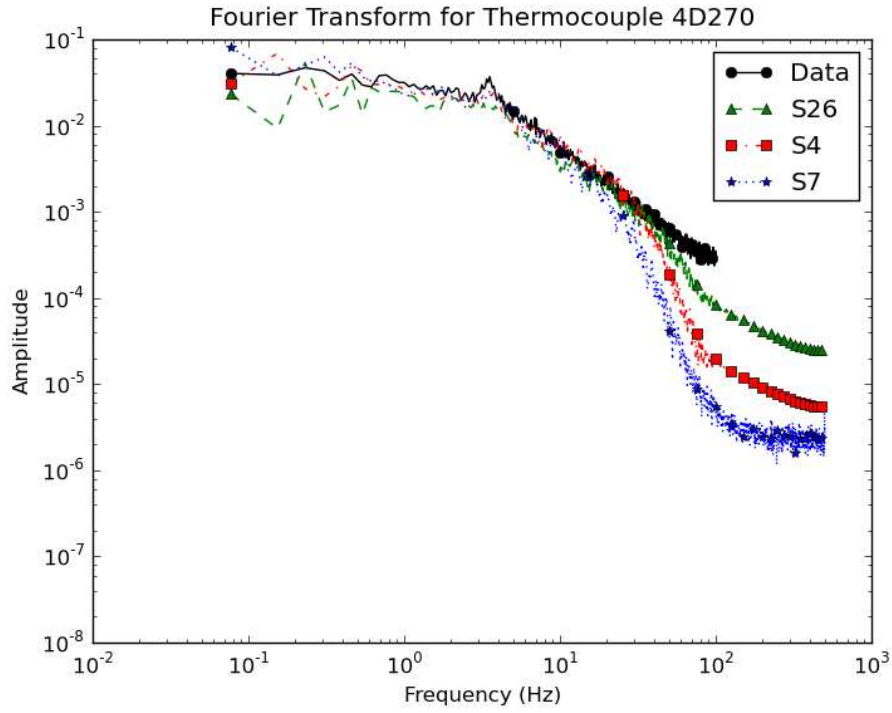


Figure 37: Closer Data Match with Fewer Volumes

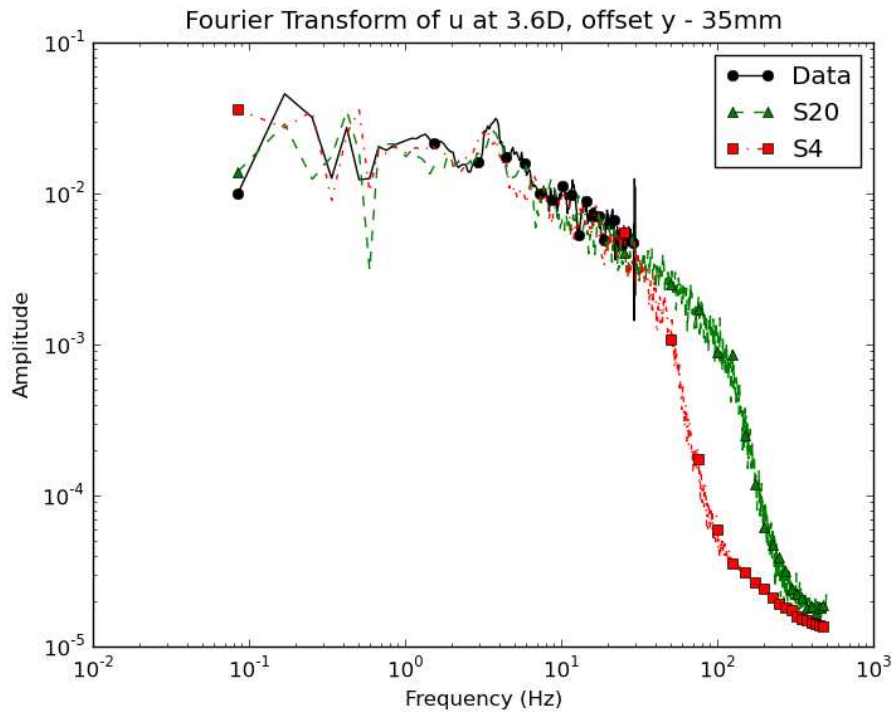
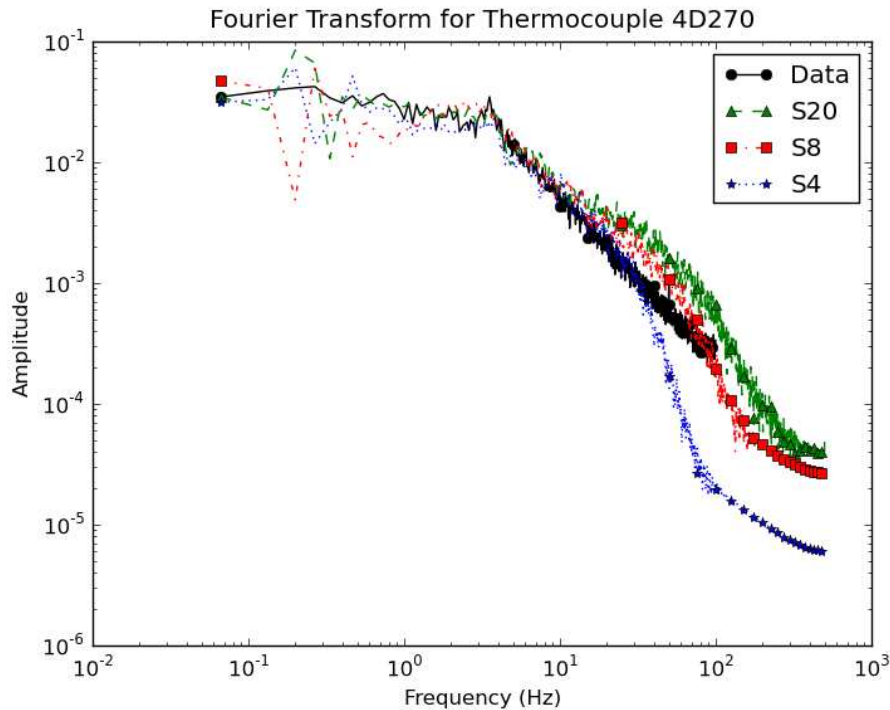


Figure 38 Fourier Spectrum for u



**Figure 39 Results for 6, 13, and 70 Million Volumes**

## **Conclusions**

Results from the Fourier analysis confirmed the observation made for time averaged behavior that SAS-SST has some significant problems with this benchmark. Submissions using this turbulence model did not do well enough matching spectral peaks to be included in Table 3. Hopefully some of the participants using this approach will perform follow-up studies to understand the source of problems and provide guidelines for future use.

The relationship noted between number of computational volumes and ranking in Tables 1 and 2 did not hold in Table 3. Insufficient information is available to decide whether this is a question of care in nodalization, or sensitivity of flow oscillation modes to nodalization or boundary conditions. Perhaps enough participants will publish results of post-benchmark sensitivity studies to improve understanding of simulation behavior and aid in creation of best practice guidelines for this class of problem.

Two major lessons were learned during synthesis of benchmark results worth noting. It was very difficult for participants to catch minor discrepancies between files submitted and file formats specified for the benchmark. However, minor discrepancies generally halted the automated processing of results, and required significant time to correct. The script driving production of plots should have been completed early in the process and provided to participants before they submitted data files, to guarantee compatibility of files with the script. In addition information submitted on general features of calculations did not always follow the requested list of basic information, and as seen above the basic list was incomplete.

Future benchmarks should consider providing a sample report in addition to the list of required information. More time should be spent designing requests for a more detailed description of spatial discretization.

## ***References***

Y. Odemark, T. M. Green, K. Angele, J. Westin, F. Alavyoon, and S. Lundström. “High-Cycle Thermal Fatigue in Mixing Tees: New Large-Eddy Simulations Validated Against New Data Obtained by PIV in the Vattenfall Experiment,” Proceedings of the 17<sup>th</sup> International Conference on Nuclear Engineering, Brussels, July 2009.